JCTC Journal of Chemical Theory and Computation

Article

pubs.acs.org/JCTC

Transition State Search Using a Guided Direct Inversion in the Iterative Subspace Method

Joseph W. May,[†] Jeremy D. Lehner,[†] Michael J. Frisch,[‡] and Xiaosong Li*[,†]

[†]Department of Chemistry, University of Washington, Seattle, Washington 98195, United States

[‡]Gaussian Inc., 340 Quinnipiac St, Bldg 40, Wallingford, Connecticut 06492, United States

ABSTRACT: A transition state optimization method using a guided energy-represented direct inversion in the iterative subspace (gEn-DIIS) algorithm is introduced and compared with the quasi-Newton rational function optimization (RFO) method. A hybrid technique that employs a combination of RFO and guided DIIS methods at various stages of convergence is presented. A set of test molecules is optimized for comparison using the hybrid method with gEn-DIIS and the traditional RFO methods. The gEn-DIIS method presented here exhibits fast optimization and is shown to be advantageous for difficult optimizations where the reaction path is flat.

1. INTRODUCTION

Molecular geometry optimization underlies any computational chemistry study by providing characteristic stationary point structures and energies on potential energy surfaces (PESs). The valleys or minima along the PES correspond to reactants, intermediates, and products. The reaction valley connecting two minima of the potential energy surface can be represented by the so-called reaction path, and first-order saddle points (where the second-order energy variation is positive with respect to all the coordinates except one, along which the variation is negative) give rise to transition states (TS). Well-characterized TS structures are essential for computing reaction barriers and reaction rates. Unfortunately, the landscape of the PES is not known during an optimization, thus requiring the use of various tools for exploring the PES and locating the stationary points. Among the most widely used tool in optimization is the Newton−Raphson method and its many variations,[1] including the rational function optimization (RFO)[2,3] and the trust radius method (TRM).[4−10] These techniques make use of the gradient and the Hessian of the PES to get information regarding the slope and local curvature at a given point along the PES. However, explicit computation of the Hessian can be unworkable for larger systems.

Least-squares minimization schemes, such as the direct inversion in the iterative subspace (DIIS),[11,12] have proven efficient at converging wave functions[11−15] and molecular geometries.[16,17] As applied to geometry optimization, the DIIS method computes a new geometry closer to the stationary point by interpolating/extrapolating a set of position vectors obtained from previous steps such that the estimated error associated with the new position is at a minimum. The error from each step is usually estimated from the RFO step (RFO−DIIS),[17] $\Delta\mathbf{x} = -(\mathbf{H} - \lambda\mathbf{I})^{-1}\cdot\mathbf{g}$, but alternate methods have used an energy representation (En-DIIS)[18,19] of the local PES in the vicinity of previously computed points to estimate the error. Furthermore, a hybrid optimization scheme that combines the benefits of RFO, RFO−DIIS, and En-DIIS has been shown to give fast and smooth convergence for optimizing to a minimum.[18]

Unlike a geometry minimization, in which all coordinates are treated equally, a TS search identifies a particular linear combination of coordinates, the reaction pathway, along which the energy is to be maximized. While the methods outlined above can successfully locate minima on a PES, the success of a TS optimization strongly depends on the researcher's chemical intuition in providing a suitable initial guess for the structure. This difficulty arises from the small radius of the quadratic region about the stationary point compared to that of an equilibrium structure.[1] Additionally, an accurate Hessian matrix is required and must contain an eigenvector with a negative eigenvalue that corresponds to the reaction pathway. For small systems in which movement along only a single coordinate gives rise to the TS, coordinate driving[20,21] and eigenvector following[2,22−24] algorithms have proven successful. Linear and quadratic synchronous transit (LST and QST)[25,26] and synchronous transit-guided quasi-Newton (STQN)[27] methods have provided a means for determining a TS starting structure by initially finding the maximum point along a path interpolated between the reactant and product minima. Path optimization[28] or chain-of-states methods[29] such as the elastic band theory[30] have been successful at not only locating TS structures but also elucidating the reaction path connecting the reactant and product molecules. The nudged elastic band (NEB) method[31−35] and the growing strings method[36,37] both minimize the energy of a series of points (referred to as images) along an interpolated pathway connecting two minima. The cost of the many energy and derivative calculations required to minimize all the images makes these methods undesirable for larger systems. More recently, Jensen has proposed the use of empirical force fields for generating PESs of the reactant and product molecules and identifying the minimum along the seam of their intersection.[38]

In this work, we introduce a guided energy-represented DIIS (gEn-DIIS) method for TS search. We also propose a hybrid

Special Issue: Berny Schlegel Festschrift

Received: August 8, 2012
Published: August 29, 2012

ACS Publications © 2012 American Chemical Society

optimization scheme that makes use of the RFO, RFO−DIIS, and En-DIIS methods at various stages of the optimization. We employ a weighting factor in the DIIS optimization to rapidly reduce the error along the reaction pathway. This guided DIIS method continues to benefit from the speed of local search methods while making use of the unique nature of the TS structure.

2. METHODOLOGY

Within the RFO scheme, the optimization step taken in the DIIS method can be written as

$$\mathbf{R}_{k+1} = \mathbf{R}_k^* + \Delta\mathbf{R}_k^* = \sum_{i=1}^{k} c_i\mathbf{R}_i - \sum_{i=1}^{k} c_i(\mathbf{H} - \xi)^{-1}\cdot\mathbf{g}_i \tag{1}$$

In eq 1, the first and second terms, $\mathbf{R}_k^* = \Sigma_{i=1}^k c_i\cdot\mathbf{R}_i$ and $\Delta\mathbf{R}_k^* = -\Sigma_{i=1}^k c_i\,(\mathbf{H} - \xi)^{-1}\cdot\mathbf{g}_i$, are the linear and quadratic steps obtained from extrapolation/interpolation of the previous vectors and RFO optimization steps, respectively. The set of coefficients $\{c_i\}$ minimize an error function in the multidimensional least-squares framework. In the context of geometry optimization, the error function can be a measure of energy ΔE, gradient $\mathbf{g}$, or optimization step $\Delta\mathbf{R}$. The DIIS scheme can be written in matrix form as

$$\begin{pmatrix} a_{1,1} & \cdots & a_{1,k} & 1 \\ \vdots & \ddots & \vdots & \vdots \\ a_{k,1} & \cdots & a_{k,k} & 1 \\ 1 & \cdots & 1 & 0 \end{pmatrix}\begin{pmatrix} c_1 \\ \vdots \\ c_k \\ \lambda \end{pmatrix} = \begin{pmatrix} 0 \\ \vdots \\ 0 \\ 1 \end{pmatrix} \tag{2}$$

where λ is the Lagrangian multiplier that satisfies the constraint $\Sigma_{i=1}^k c_i = 1$. With no constraint on the sign of c_i, the DIIS solution gives rise to either extrapolation or interpolation in the search space. When the molecular geometry is far from convergence, extrapolations can lead to erroneously large steps away from the optimized geometry. To ensure optimization stability, an enforced interpolation constraint, $c_i > 0$, is added when solving eq 2 (for further details, see ref 14).

In our previous work,[15,19] we derived an energy-represented least-squares minimization method where the error function is defined as

$$f = \frac{1}{2}\sum_{i,j=1}^{k} c_ic_j\left[\frac{1}{2}(\mathbf{g}_i^T\cdot\mathbf{H}^{-1}\cdot\mathbf{g}_i + \mathbf{g}_j^T\cdot\mathbf{H}^{-1}\cdot\mathbf{g}_j) + (\mathbf{R}_i^T\cdot\mathbf{g}_j + \mathbf{R}_j^T\cdot\mathbf{g}_i - \mathbf{R}_i^T\cdot\mathbf{g}_i - \mathbf{R}_j^T\cdot\mathbf{g}_j)\right] \tag{3}$$

In eq 3, the first set of terms in the bracket gives rise to energy errors of the search space relative to the minimum of the local quadratic surface. The second set of terms describes variations in energy for changes of coordinate and gradient vectors within the search space. As the error function in eq 3 is quadratic with respect to the $\{c_i\}$, minimization can be performed in a least-squares sense using eq 2, where

$$a_{i,j} = \frac{1}{2}(\mathbf{g}_i^T\cdot\mathbf{H}^{-1}\cdot\mathbf{g}_i + \mathbf{g}_j^T\cdot\mathbf{H}^{-1}\cdot\mathbf{g}_j) + (\mathbf{R}_i^T\cdot\mathbf{g}_j + \mathbf{R}_j^T\cdot\mathbf{g}_i - \mathbf{R}_i^T\cdot\mathbf{g}_i - \mathbf{R}_j^T\cdot\mathbf{g}_j) \tag{4}$$

An optimization scheme using eqs 1−4 will be referred to as En-DIIS. This method has consistently shown smooth and fast optimization for locating local minimum structures.[15] When the subject of interest is a transition state instead of a minimum, one of the eigenvalues of the Hessian needs to be of negative sign. In other words, the optimizer searches for the maximum along one and only one vector (the reaction path), while minimizing the energy along the remaining coordinates. In order to maintain the correct optimization direction, the TS search scheme introduced here is performed in the eigenspace of the Hessian, where the number of negative eigenvalues can be verified as the optimization proceeds. The gradient and coordinate vectors may be transformed using the Hessian eigenvectors as such

$$\mathbf{H} = \mathbf{C}\cdot\varepsilon\cdot\mathbf{C}^{\dagger} \tag{5}$$

$$\tilde{\mathbf{g}}_i = \mathbf{C}^T\cdot\mathbf{g}_i \tag{6}$$

$$\tilde{\mathbf{R}}_i = \mathbf{C}^T\cdot\mathbf{R}_i \tag{7}$$

where ε is a diagonal matrix containing the force constants. In the normal coordinate system, eq 4 becomes

$$\tilde{a}_{i,j} = \frac{1}{2}(\tilde{\mathbf{g}}_i^T\cdot\varepsilon^{-1}\cdot\tilde{\mathbf{g}}_i + \tilde{\mathbf{g}}_j^T\cdot\varepsilon^{-1}\cdot\tilde{\mathbf{g}}_j) + (\tilde{\mathbf{R}}_i^T\cdot\tilde{\mathbf{g}}_j + \tilde{\mathbf{R}}_j^T\cdot\tilde{\mathbf{g}}_i - \tilde{\mathbf{R}}_i^T\cdot\tilde{\mathbf{g}}_i - \tilde{\mathbf{R}}_j^T\cdot\tilde{\mathbf{g}}_j) \tag{8}$$

There are several advantages to using eq 8 for a TS search. The optimization direction can be well maintained by choosing the correct sign of the eigenvalues ε at each step. In addition, the weight of each normal mode in the least-squares minimization scheme can be controlled. Inspired by the nature of the TS search, we propose the following equation as a guided optimization scheme that weighs the reaction path (the eigenvector with a negative eigenvalue) heavier than the rest of the coordinates within the least-squares framework:

$$\begin{aligned}\tilde{a}_{i,j} = {} & \frac{1}{2}\sum_{\varepsilon_\mu<0} S\cdot(\tilde{g}_{\mu,i}\cdot\varepsilon_\mu^{-1}\cdot\tilde{g}_{\mu,i} + \tilde{g}_{\mu,j}\cdot\varepsilon_\mu^{-1}\cdot\tilde{g}_{\mu,j} + \tilde{R}_{\mu,i}\cdot\tilde{g}_{\mu,j} \\ & + \tilde{R}_{\mu,j}\cdot\tilde{g}_{\mu,i} - \tilde{R}_{\mu,i}\cdot\tilde{g}_{\mu,i} - \tilde{R}_{\mu,j}\cdot\tilde{g}_{\mu,j}) \\ & + \sum_{\varepsilon_\nu>0}(\tilde{g}_{\nu,i}\cdot\varepsilon_\nu^{-1}\cdot\tilde{g}_{\nu,i} + \tilde{g}_{\nu,j}\cdot\varepsilon_\nu^{-1}\cdot\tilde{g}_{\nu,j} + \tilde{R}_{\nu,i}\cdot\tilde{g}_{\nu,j} \\ & + \tilde{R}_{\nu,j}\cdot\tilde{g}_{\nu,i} - \tilde{R}_{\nu,i}\cdot\tilde{g}_{\nu,i} - \tilde{R}_{\nu,j}\cdot\tilde{g}_{\nu,j})\end{aligned} \tag{9}$$

In eq 9, μ and ν index eigenvectors/eigenvalues of the Hessian and S is the weighting factor for the reaction path. The first sum collects errors associated with the reaction path with $\varepsilon_\mu < 0$, whereas the second sum evaluates the remaining vectors associated with a downhill minimization. When $S > 1$, the optimizer prioritizes locating the reaction path vector over minimizing the coordinates that are orthogonal to the reaction path. The following test cases will show that this method quickly locates the transition vector while minimizing the remaining coordinates.

3. BENCHMARK AND DISCUSSION

Optimizations were carried out on an SGI Atlix 450 workstation (Intel dual-core Itanium 1.6 GHz with 48 GB of RAM) using the development version of the GAUSSIAN program[39] with the addition of the guided En-DIIS algorithm presented here for TS optimization. For all methods tested here, the optimization is considered converged when the maximum component of the gradient vector is less than 4.5×10^{-4} au, the root-mean-square (RMS) gradient is less than $3 \times$

Table 1. Comparison of the Computational Costs for Quasi-Newton RFO and Guided En-DIIS Transition State Optimization Methods on Selected Test Molecules at the HF/3-21G Level of Theory

		RFO		gEn-DIIS	
	E^a (au)	N^b	ν (cm^{-1})	N^b	ν (cm^{-1})
$CH_3CHO \rightarrow CH_2CHOH$	−151.913 10	8	−2513.0	7	−2513.0
$H_2CO \rightarrow H_2 + CO$	−113.050 03	6	−2213.0	6	−2213.3
$SiH_2 + H_2 \rightarrow SiH_4$[c]	−289.565 03	8	−1714.9	7	−1714.5
$H_3CO \rightarrow H_2COH$[c]	−113.621 92	12	−1721.9	15	−1720.9
$CH_3 + HF \rightarrow CH_4 + F$[c]	−138.779 63	5	−2897.5	5	−2897.6
$CH_3CH_2F \rightarrow CH_2CH_2 + HF$	−176.984 53	13	−2094.5	14	−2094.0
Diels−Alder reaction[c,d]	−231.603 21	6	−818.2	6	−818.2
Claisen rearrangement[c,e]	−267.238 59	18	−763.2	17	−763.3
Ene reaction[d,f]	−193.942 54	23	−1690.2	29	−1689.6

[a]Final energy. [b]Number of optimization steps. [c]Initial structures taken from ref 27. [d]$CH_2CH_2 + CH_2CHCHCH_2 \rightarrow C_6H_{10}$. [e]$CH_2CHCH_2OCHCH_2 \rightarrow CH_2CHCH_2CH_2CHO$. [f]$CH_2CH_2 + CH_2CHCH_3 \rightarrow CH_2CHCH_2CH_2CH_3$.

10^{-4} au, the maximum component of the displacement is less than 1.8×10^{-3} au, and the RMS displacement is less than 1.2×10^{-3} au. The following optimization strategies are used in the benchmark tests: (1) the analytical Hessian is computed at the first step, and subsequent Hessians are updated using Bofill's weigted update of the Powell and Murtagh−Sargent method;[40] (2) if there is more than one negative eigenvalue associated with the initial geometry, the RFO approach is used until only one negative force constant remains; (3) when the RMS gradient is greater than 10^{-3} au, the weight factor S in eq 9 is set to be equal to the total number of nuclear degrees of freedom; and (4) when the RMS gradient is less than 10^{-3} au, and the optimization step is considered to be in the quadratic region of the PES, standard RFO−DIIS,[16,17] without any weighting factor ($S = 1$), is used until convergence is reached. For all test cases considered below, the weighting factor S in eq 9 was set equal to the number of nuclear degrees of freedom so as to weight the error along the reaction path equally with the combined weight of all the other coordinates. Alternate values of S were also considered and revealed this to be the optimal choice for the weighting factor.

Table 1 lists TS optimization performance using the guided En-DIIS method. For all small molecule test cases, the method is able to successfully locate the TS. The final TS structures and imaginary frequencies are in excellent agreement with those obtained using the RFO approach. While the guided En-DIIS method exhibits consistently excellent performance on these well-studied test cases, the next two test cases are considered challenging for a TS search algorithm.

The TS (structure given in Figure 1) in the electrocyclic ring-opening of [12]annulene (cyclododecahexane) is associated with a relatively flat reaction path (small absolute value of the negative force constant at the TS). Additionally, the PES of multiple coordinates that are perpendicular to the reaction path are also very flat (with two positive eigenvalues less than 10^{-2} au). Such conditions can often *frustrate* a TS search algorithm. Figure 1 compares the TS optimization of [12]annulene using the algorithm introduced above to the traditional RFO method. In this TS search, the guided En-DIIS method exhibits multiple large oscillations, which seem uncharacteristic because DIIS is known to have smooth optimization behavior.[15,19] When the reaction path vector is weighed heavier in the minimization scheme, as in the guided En-DIIS approach, the optimal conditions are not satisfied for optimizing the remaining coordinates. As a result, the total energy and total RMS

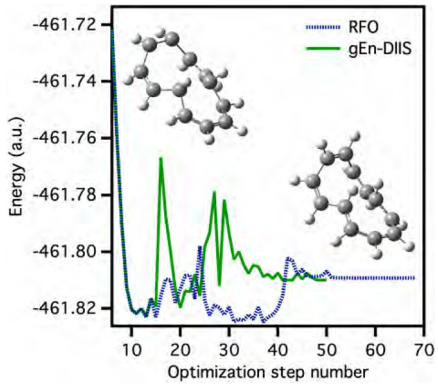

Figure 1. Comparison of transition state optimization methods for the electrocyclic ring-opening of [12]annulene at the B3LYP/3-21G level of theory. The structure on the left corresponds to the initial structure used in the RFO and guided En-DIIS (gEn-DIIS) optimizations, and the structure on the right corresponds to the optimized transition state structure obtained from the gEn-DIIS method.

gradient can exhibit large oscillations due to nonoptimal pathways for the majority of coordinates during the early stage of optimization. However, hidden in such seemingly unproductive oscillations is the algorithm minimizing errors associated with the most important transition state vector and climbing uphill along the reaction path coordinate. Figure 2 shows the total RMS force, and the inset shows the value of the force of the TS vector at each optimization step. While the total RMS force seems unstable with large oscillations, the force of the TS vector is minimized toward the maximum using the guided En-DIIS method. Figure 1 also suggests that the RFO method takes on a different TS optimization pathway than that of the guided En-DIIS approach. As the guided En-DIIS does not choose to fully optimize the majority of coordinates during the early stage of the optimization process, the total energy never reaches as low as that of the RFO approach until the end due to the nonoptimal minimization pathways for nonreaction-path coordinates. For TS optimization, this happens to be an ideal situation because optimizing the nonreaction-path coordinates when the TS vector is still undetermined or unstable is often unproductive. In this test case, the guided En-DIIS shows a speedup of 30% compared to RFO.

While most TS search methods show success on small test cases, large molecules with many nuclear degrees of freedom

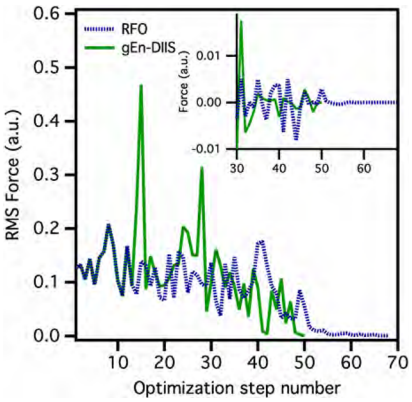

Figure 2. Root-mean-square (RMS) of the force for the transition state optimization of the elctrocyclic ring-opening of [12]annulene at the B3LYP/3-21G level of theory. Inset: Value of the first element of the gradient corresponding to the force along the reaction pathway of this transition state optimization.

often pose great difficulty. Figure 3 shows the TS structure of the proton diffusion pathway in a 1.2 nm CdSe nanocrystal.

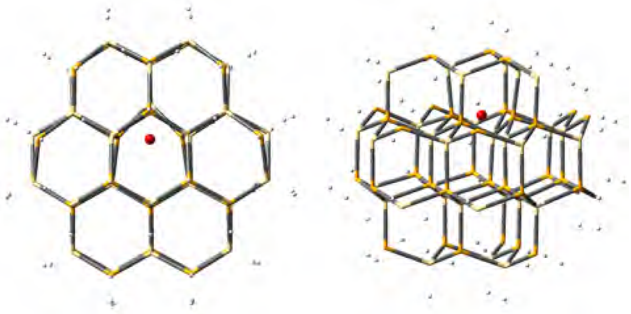

Figure 3. Transition state structure of a proton diffusion pathway in a 1.2 nm CdSe nanocrystal optimized using the guided En-DIIS method at the PBE1PBE/LANL2DZ level of theory. The position of the diffused hydrogen atom is given by the red dot.

Due to strongly coupled reaction paths and an extremely flat PES (with six positive eigenvalues less than 10^{-3} au) at the TS associated with the proton, RFO converged to a second-order saddle point after 70 optimization steps. On the other hand, the guided En-DIIS method converges to the TS structure after 66 optimization steps, again exhibiting fast and stable optimization for a difficult case.

4. CONCLUSION

In this work, we introduced a guided energy-represented DIIS method for molecular TS optimization. During the early stage of optimization, the errors arising from the TS vector are weighed heavier in the least-squares minimization scheme. This approach leads to quick stabilization of the transition vector before the full optimization of the nonreaction coordinates begins. Test cases show that this method exhibits fast optimization to locate the TS. In difficult cases where the reaction path is flat (a small absolute value of the force constant), this method is particularly advantageous because of its ability to stabilize the reaction coordinate in a multidimensional system. Last, it should be noted that the method presented here, in which a weighting factor is used to guide the optimization along a desired pathway, could be used in any optimization method that is carried out in the normal coordinate system, including the RFO approach.

AUTHOR INFORMATION

Corresponding Author

*E-mail: li@chem.washington.edu.

Notes

The authors declare no competing financial interest.

ACKNOWLEDGMENTS

This work was supported by the U.S. National Science Foundation (CHE-CAREER 0844999). Additional support from the Alfred P. Sloan Foundation, Gaussian Inc., and the University of Washington Student Technology Fund is gratefully acknowledged.

REFERENCES

(1) Hratchian, H. P.; Schlegel, H. B. In *Theory and Applications of Computational Chemistry: The First 40 Years*; Dykstra, C. E., Kim, K. S., Frenking, G., Scuseria, G. E., Eds.; Elsevier: Amsterdam, 2005; pp 195−259.
(2) Banerjee, A.; Adams, N.; Simons, J.; Shepard, R. *J. Phys. Chem.* **1985**, *89*, 52−57.
(3) Simons, J.; Nichols, J. *Int. J. Quantum Chem.* **1990**, *24*, 263−276.
(4) Schlegel, H. B. In *Modern Electronic Structure Theory*; Yarkony, D. R., Ed.; World Scientific: Singapore, 1995; p 459.
(5) Schlegel, H. B. In *Encyclopedia of Computational Chemistry*; Schleyer, P. v. R., Allinger, N. L., Killman, P. A., Clark, T., Schaefer, H. F., Gasteiger, J., Schreiner, P. R., Eds.; Wiley: Chichester, U. K., 1998; Vol. *2*; p 1136.
(6) Fletcher, R. *Practical Methods of Optimization*; Wiley: Chichester, U. K., 1981.
(7) Murray, W.; Wright, M. H. *Practical Optimization*; Academic: New York, 1981.
(8) Powell, M. J. D. *Nonlinear Optimization*; Academic: New York, 1982.
(9) Dennis, J. E.; Schnabel, R. B. *Numerical Methods for Unconstrained Optimization and Nonlinear Equations*; Prentice Hall: Upper Saddle River, NJ, 1983.
(10) Scales, L. E. *Introduction to Nonlinear Optimization*; Macmillam: Basingstoke, England, 1985.
(11) Pulay, P. *Chem. Phys. Lett.* **1980**, *73*, 393−398.
(12) Pulay, P. *J. Comput. Chem.* **1982**, *3*, 556−560.
(13) Cances, E.; Bris, C. L. *Int. J. Quantum Chem.* **2000**, *79*, 82−90.
(14) Kudin, K. N.; Scuseria, G. E.; Cances, E. *J. Chem. Phys.* **2002**, *116*, 8255−8261.
(15) Li, X.; Millam, J. M.; Scuseria, G. E.; Frisch, M. J.; Schlegel, H. B. *J. Chem. Phys.* **2003**, *119*, 7651−7658.
(16) Csaszar, P.; Pulay, P. *J. Mol. Struct.* **1984**, *114*, 31−34.
(17) Farkas, Ö.; Schlegel, H. B. *Phys. Chem. Chem. Phys.* **2002**, *4*, 11−15.
(18) Li, X.; Frisch, M. J. *J. Chem. Theory Comput.* **2006**, *2*, 835−839.
(19) Moss, C. L.; Li, X. *J. Chem. Phys.* **2008**, *129*, 114102.
(20) Hirsch, M.; Quapp, W. *J. Comput. Chem.* **2002**, *23*, 887−894.
(21) Crehuet, R.; Bofill, J. M.; Anglada, J. M. *Theor. Chem. Acc.* **2002**, *107*, 130−139.
(22) Simons, J.; Jorgensen, P.; Taylor, H.; Ozment, J. *J. Phys. Chem.* **1983**, *87*, 2745−2753.
(23) Cerjan, C. J.; Miller, W. H. *J. Chem. Phys.* **1981**, *75*, 2800−2806.
(24) Nichols, J.; Taylor, H.; Schmidt, P.; Simons, J. *J. Chem. Phys.* **1990**, *92*, 340−346.
(25) Halgren, T. A.; Lipscomb, W. N. *Chem. Phys. Lett.* **1977**, *49*, 225−232.
(26) Bell, S.; Crighton, J. S. *J. Chem. Phys.* **1984**, *80*, 2464−2475.
(27) Peng, C.; Schlegel, H. B. *Israel J. Chem.* **1993**, *33*, 449−454.
(28) Ayala, P. Y.; Schlegel, H. B. *J. Chem. Phys.* **1997**, *107*, 375−384.
(29) Pratt, L. R. *J. Chem. Phys.* **1986**, *85*, 5045−5048.

(30) Elber, R.; Karplus, M. *Chem. Phys. Lett.* **1987**, *139*, 375−380.
(31) Henkelman, G.; Uberuaga, B. P.; Jonsson, H. *J. Chem. Phys.* **2000**, *113*, 9901−9904.
(32) Henkelman, G.; Jonsson, H. *J. Chem. Phys.* **2000**, *113*, 9978−9985.
(33) Maragakis, P.; Andreev, S. A.; Brumer, Y.; Reichman, D. R.; Kaxiras, E. *J. Chem. Phys.* **2002**, *117*, 4651−4658.
(34) Trygubenko, S. A.; Wales, D. J. *J. Chem. Phys.* **2004**, *120*, 2082−2094.
(35) Chu, J.-W.; Trout, B. L.; Brooks, B. R. *J. Chem. Phys.* **2003**, *119*, 12708−12717.
(36) Peters, B.; Heyden, A.; Bell, A. T.; Chakraborty, A. *J. Chem. Phys.* **2004**, *120*, 7877−7886.
(37) Goodrow, A.; Bell, A.; Head-Gordon, M. *J. Chem. Phys.* **2008**, *129*, 174109.
(38) Jensen, F. *J. Chem. Phys.* **2003**, *119*, 8804−8808.
(39) Frisch, M. J.; Trucks, G. W.; Schlegel, H. B.; Scuseria, G. E.; Robb, M. A.; Cheeseman, J. R.; Scalmani, G.; Barone, V.; Mennucci, B.; Petersson, G. A.; Nakatsuji, H.; Caricato, M.; Li, X.; Hratchian, H. P.; Izmaylov, A. F.; Bloino, J.; Zheng, G.; Sonnenberg, J. L.; Liang, W.; Hada, M.; Ehara, M.; Toyota, K.; Fukuda, R.; Hasegawa, J.; Ishida, M.; Nakajima, T.; Honda, Y.; Kitao, O.; Nakai, H.; Vreven, T.; Montgomery, J. A., Jr.; Peralta, J. E.; Ogliaro, F.; Bearpark, M.; Heyd, J. J.; Brothers, E.; Kudin, K. N.; Staroverov, V. N.; Keith, T.; Kobayashi, R.; Normand, J.; Raghavachari, K.; Rendell, A.; Burant, J. C.; Iyengar, S. S.; Tomasi, J.; Cossi, M.; Rega, N.; Millam, J. M.; Klene, M.; Knox, J. E.; Cross, J. B.; Bakken, V.; Adamo, C.; Jaramillo, J.; Gomperts, R.; Stratmann, R. E.; Yazyev, O.; Austin, A. J.; Cammi, R.; Pomelli, C.; Ochterski, J. W.; Martin, R. L.; Morokuma, K.; Zakrzewski, V. G.; Voth, G. A.; Salvador, P.; Dannenberg, J. J.; Dapprich, S.; Parandekar, P. V.; Mayhall, N. J.; Daniels, A. D.; Farkas, Ö.; Foresman, J. B.; Ortiz, J. V.; Cioslowski, J.; Fox, D. J. *Gaussian Development Version*, Revision H.21; Gaussian Inc.: Wallingford, CT, 2012.
(40) Bofill, J. M. *J. Comput. Chem.* **1994**, *15*, 1−11.